NUKLEONIKA 2009;54(4):223–226

ORIGINAL PAPER

The implantation profile of positrons emitted in beta plus decay of ^{48}V in water

Jerzy Dryzek,
Paweł Horodek,
Ewa Dryzek

Abstract. The experimental technique based on scanning of positron implantation profile, hereafter referred to as the DSIP is used for the determination of linear absorption coefficient for positrons emitted from a ^{48}V source into water. This coefficient is equal to $1/(299 \pm 62)$ μm^{-1}. The determined value is in agreement with the one obtained from the computer simulations using the well known EGS nrc 4.0 and GEANT4 codes. The experimental technique was used for the determination of linear absorption coefficients for ^{48}V positrons in materials of biological origin. The presented data can be useful for PET studies because of similarities of the ^{18}F and ^{48}V positron implantation profiles.

Key words: positron implantation range in water • V-48 positron emitter

J. Dryzek✉
The Henryk Niewodniczański Institute
of Nuclear Physics,
Polish Academy of Sciences,
152 Radzikowskiego Str., 31-342 Kraków, Poland
and Institute of Physics,
Opole University,
48 Oleska Str., 45-052 Opole, Poland,
Tel.: +48 12 662 8370, Fax: +48 12 662 8458,
E-mail: jerzy.dryzek@ifj.edu.pl

P. Horodek, E. Dryzek
The Henryk Niewodniczanski Institute
of Nuclear Physics,
Polish Academy of Sciences,
152 Radzikowskiego Str., 31-342 Kraków, Poland

Received: 11 February 2009
Accepted: 20 July 2009

The radionuclide ^{48}V is employed in many research areas from biology [2] to materials science [1]. Additionally, it is recommended for the intravascular brachytherapy (IVBT) [7] and may be used as an alternative to ^{68}Ge/^{68}Ga for transmission scanning in PET [9]. These are due to the positron and emergent photons nuclear emission and short half-lifetime (15.97 d). The ^{48}V nucleus decays to the excited states of ^{48}Ti nucleus via several electron capture branches and three β^+ decay channels. The main channel (49.5%) is the β^+ decay for which the end-point energy is equal to 695 keV, the next one (0.8%) with the end-point energy equal to 2001 keV and the minor channel (0.0001%) with the end-point energy equal to 569 keV. The energies of the main gammas emitted from the excited states of ^{48}Ti nucleus are equal to 984 keV (99.9%) and 1312 keV (97.5%).

The energy end-point of β^+ decay of the widely employed PET radionuclide, i.e., ^{18}F, is equal to 635 keV and it is close to the energy end-point of the main β^+ decay of the ^{48}V radionuclide. The ^{48}V distributed in the solid target is easy to handle in comparison to ^{18}F which is a gas radionuclide. We employ this feature to determine the positron implantation profile in water and other biological tissues and the results may be extrapolated for ^{18}F.

The positron range is an important factor, limiting the spatial resolution of PET (positron emission tomography), but this factor is deduced mainly from the Monte Carlo simulations [10, 11]. Its experimental verification is necessary. However, in our work we intend also to

support our measurements with the Monte Carlo simulations, using the EGS nrc 4 and GEANT4 codes.

For the preparation of the ^{48}V radionuclide, we used a titanium 120 μm thick plate of size 10 × 10 mm, (purity 99.6+%, purchased from Nilaco). The plate was a target for the proton beam of energy up to 30 MeV. The target was irradiated during 2 h with a 0.5 μA internal proton beam in the AIC-144 cyclotron at the Henryk Niewodniczański Institute of Nuclear Physics of the Polish Academy of Sciences [12]. The target was used for the measurements after seven days after irradiation allowing the short living impurities to decay. The activity of the source used in experiments was ca. 0.2 mCi.

We performed our measurements using a method called depth scanning of positron implantation profile (DSIP) [4]. In that method we employ the fact that annihilation photons tag the end of positron implantation path. The positron diffusion length is much smaller and is negligible in our consideration. The detection of the annihilation photons was performed by an HpGe detector located behind the 60 μm wide slit in a 10 cm thick shield made from a tungsten-based heavy metal (TRIAMET with 95% tungsten). The activated titanium plate fixed to a plexi plate was immersed into water and placed in the front of the collimator as shown in Fig. 1. The plexi plate ensured position of the thin titanium plate parallel to the slit. The water container was located on the table which could be shifted precisely in the direction perpendicular to the slit. Thanks to this, the HpGe detector registered gamma quanta coming from different specified regions of the water container. The sequenced measurements of the photon spectra as a function of position of the table with the water container and the activated titanium plate allow us to scan regions close to the plate. Each spectrum was measured during 1 h. A positron emitted form the titanium plate was injected into water and then traversed a certain distance. Finally, it annihilated with a random electron and two annihilation photons were emitted indicating the point position of that process. Registering these photons in the function of distance or depth from the emitter, one can obtain the positron implantation profile in water. More details of the experimental apparatus employed are given in Ref. [4]. The measurements were performed also for materials of biological origin listed in Table 1. In the case of non-liquid materials the specimens were cut in the form of right square prism

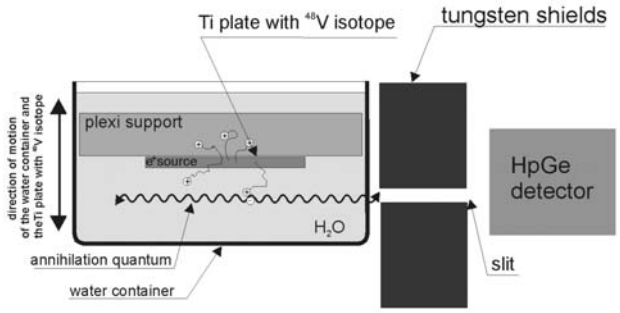

Fig. 1. A layout of the experimental setup (not in the scale). The Ti plate with the positron emitter ^{48}V is glued to the plexi support and both are immersed into water. The water container can be precisely moved in the front of the tungsten slit. Behind the slit, the HpGe detector is located which observes the emitted gamma photons.

Table 1. The measured values of the reciprocal of the linear absorption coefficient for the positrons emitted from a ^{48}V source into water and different materials of biological origin

	α^{-1} (μm)
Water	299±62
Vegetable oil	230±46
Chicken breast	118±51
Ham	139±43
Pork fat	97±30

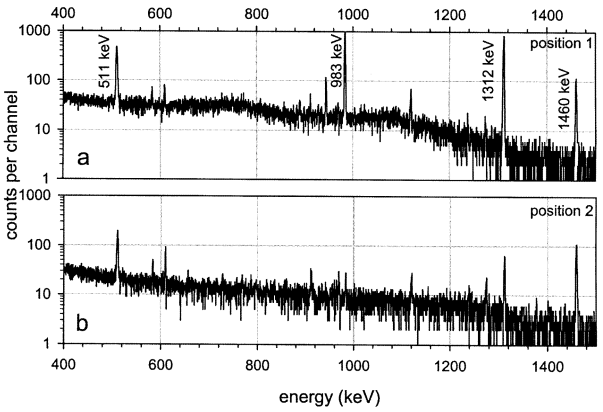

Fig. 2. The net spectra recorded by the HpGe detector located behind the slit in two selected positions of the water container. Part (a) of the figure is for the irradiated Ti plate positioned against the slit. Part (b) of the figure is for the irradiated Ti plate positioned outside the slit. The difference of the intensities of the nuclear lines originated in the titanium plate due to the decay of the ^{48}V nuclei and the intensity of the annihilation line 511 keV is visible. The spectrum acquisition times were equal.

10 × 10 × 5 mm and placed directly on the titanium plate. The plexi support with the titanium plate and specimen were immersed in distilled water.

The raw energy spectra of photons detected by the HpGe detector for two positions of the table with the plate related to the slit are presented in Fig. 2. The annihilation line and other gamma lines emitted from the excited states of ^{48}Ti are shown in this figure. It is worth noticing that changes of intensities of the lines for two different positions of the table are visible. In the measurement, the gross area under these lines is monitored as the function of the position of the table. In Fig. 3 we present the dependency obtained when the plate is immersed into distilled water. In Fig. 3a the gross area for two gammas of energy 983 keV and 1312 keV are presented and in Fig. 3b the gross area under the annihilation peak (511 keV) is depicted. The latter actually monitors the implantation depth of positrons only.

There are three parts tagged in Fig. 3b. In the left part, the region of water is represented. In the right part, the region of the plexi and the middle part (hatched area), the region where the titanium plate was located, are depicted. Only in the latter region the intensities of the gamma photons are significant, Fig 3a. The total thickness of the titanium region is about 240 μm, and it is the double of the thickness of the titanium plate. Similar effect, i.e. an increase of the thickness of the active region in comparison to the real thickness, was

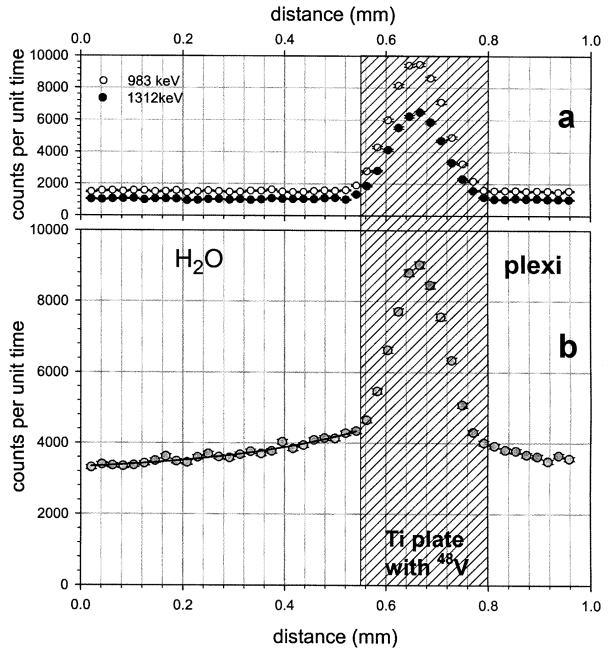

Fig. 3. Total number of counts (gross area) in the nuclear lines: 983 keV and 1312 keV (a) and annihilation line 511 keV (b) as a function of the position of water container with the activated titanium plate. The hatched part corresponds to the region with the activated Ti plate and the left part corresponds to the region with water. The solid line represents the fitted exponential decay function describing the positron implantation profile, the linear absorption coefficient is one of the adjustable parameters.

already reported in Ref. [4] for another source, e.g. ^{22}Na, enveloped in a 7 μm kapton foil. We think that this is due to the multiple Compton scattering of photons in the slit, which can reach detector even when the plate is not geometrically located behind the slit. The geometrical inaccuracies are not excluded. The most interesting is the decrease of the measured number of counts in the part where water is represented, i.e. the left part in Fig. 3b. The high level of background in this region originated in the high amount of gamma photons emitted from the ^{48}Ti excited states. Nevertheless, the expected exponential decay of the number of counts in this region is well recognized. Certainly, this is due to the positrons, which penetrate water and finally annihilate with electrons, and this process is indicated by the emission of two photons, one of which is detected. It is well known that before annihilation positrons spend some time walking randomly with thermal energies, nevertheless the average distance which they traverse is about 0.1 μm. This is much less than the distance in the implantation process. Thus, the points in the left part of Fig. 3b, represent the measured histogram of the x-coordinates of positron annihilation point distribution. For the data analysis, we consider the approach for which distribution is described by the simple exponential function:

$$P(x) = C \exp(-\alpha x) + Bg, \tag{1}$$

where C, Bg and α are the adjustable parameters used in the fitting procedure. The α parameter is the linear absorption coefficient. We are aware that the distribution exhibits much more complex behavior, and this was discussed in Refs. [5, 6]. Nevertheless, the high background in the measurements did not allow us to distinguish more details and we postulate that Eq. (1) is sufficient for the description of our data. Indeed, the solid line in Fig. 3b represents the best fit of relation (1) to the experimental points in the left part, (the direction of the x-axis is reversed) and follows the points quite well. The reciprocal of the linear absorption coefficient is equal to 299±62 μm and it is for positrons emitted from the ^{48}V radionuclide into distilled water. The high background, which limits the accuracy in determination of the coefficient, is induced by the presence of Compton scattered gamma photons originated from the excited state of the ^{48}Ti nuclei and ^{46}Sc. The latter are produced in the (p,X) reactions on other natural titanium isotopes: ^{46}Ti(8.2%), ^{47}Ti(7.4%), ^{49}Ti(5.4%), ^{50}Ti(5.2%). Additionally, only 49.9% of decay modes from ^{48}V to exited states of ^{48}Ti are accompanied by the β^+ decay. The background can be reduced if another annihilation photon could be used for triggering the measured spectrum. In our future experiments we plan to improve our setup in that way.

The obtained value may be compared with the theoretical value calculated using the Monte Carlo simulation with EGS nrc 4 code system. The EGS (electron gamma-shower) system of computer codes is a general-purpose package for the Monte Carlo simulation of the coupled transport of electrons (positrons) and photons in an arbitrary geometry [13]. We assumed the identical procedure as it was applied in Ref. [6], but this time positrons were produced in the β^+ decay of ^{48}V and then implanted into water. In Fig. 4a the histogram (dark grey) of the x-coordinates of positron annihilation point distribution is depicted. Two β^+ plus decays were taken into account and the minor decay with the end-point energy equal to 2001 keV causes a long range tail which is not detected in our experiment. The distribution has "cusp-like" shape, nevertheless, the exponential decay is well recognized and from that we can deduce

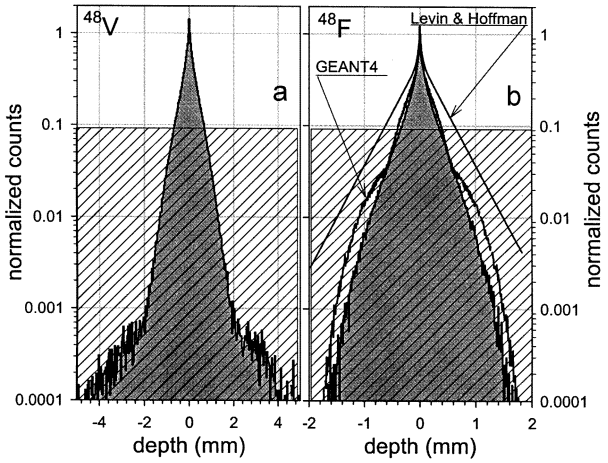

Fig. 4. The positron implantation profiles calculated using EGS nrs 4.0 code (the dark grey histograms) for positrons emitted from the ^{48}V nuclei (a) and for positrons emitted from the ^{18}F nuclei (b) in β^+ decays. In both cases the positrons emitted from the point source were injected in a full solid angle into material, i.e. water. For comparison, the solid lines in (b) represent the profiles calculated by Levin and Hoffman [10] and GEANT4 [8]. The hatched area represents the regions, which are usually not detected in experiments.

the linear absorption coefficient. The reciprocal of that coefficient is equal to 312±2 μm and it is within the accuracy of the experimental value presented above. Then, we performed identical simulations for another isotope, i.e. ^{18}F, which is important in biological applications. In Fig. 4b we depicted the histogram for the case when positrons emitted from point source of ^{18}F are injected into water. We extracted the linear absorption coefficient, whose reciprocal is equal to 231±2 μm. This value is slightly lower than that reported by other authors: 253 μm (Derenzo [3]), and 266 μm (Palmer *et al*. [11]). Levin and Hoffman [10] using their own computer codes found a similar "cusp-like" shape of the obtained distribution, which was described by the sum of two exponential functions, see Fig. 4b. In that case the distribution is broader than ours obtained using the EGS nrc 4 code. To confirm our EGS nrc 4 results we performed another simulations using a new toolkit dedicated to the simulation of interaction of energetic particle with the matter called GEANT4 [8]. The results obtained by the new code follow our previous result as shown in Fig. 4b. In Fig. 4 the hatched area tags the region which is usually hidden in real experiments due to the background and detector efficiency.

In our case the distribution has its end-point at a certain depth, which is equal ca. seven times the reciprocal of the linear absorption coefficient as it was reported in our previous papers [5, 6]. For positrons emitted from ^{18}F, and ^{18}V it is equal to ca. 1.6 and 2.1 mm, respectively. (In case of ^{48}V we neglected the long tail originated from the second β^+ decay). There is a maximal spatial extent of positron implantation profiles in water for positrons emitted from both nuclei, Fig. 4. In real experiment that value would be difficult to distinguish due to always present a certain level of background. We can argue that in the experimental techniques of detection based on scintillators and photomultipliers the maximal spatial extent of positron implantation profile is only ca. three times the reciprocal of the linear absorption coefficient. Thus, in water one should expect that the observed maximal spatial extent is ca. 0.4 mm for ^{18}F and 0.7 mm for ^{48}V positrons. In organic tissues that value can be even shorter. In Table 1 we summarize the values of the reciprocal of the linear absorption coefficient measured for other materials in the same way like for water. For materials of biological origin, the positron implantation depth is shorter than for water mainly due to the higher density.

The conclusions of the present work can be summarized as follows. The ^{48}V radionuclide obtained by the high energetic proton irradiation of the pure titanium plate is a suitable source for positron studies in liquids and other materials. The linear absorption coefficient for positrons emitted from that radionuclide in water, and determined using the DSIP method is equal to $1/(299\pm62)$ μm^{-1}. This value is in qualitative agreement with the value determined from the Monte Carlo simulation using EGS nrc 4.0 and GEANT4 codes. In materials of biological origin, the value of this coefficient is ca. twice as high as for water. The value of the ^{48}V positron end-point energy may constitute the top limitation of this quantity for the ^{18}F radionuclide widely used in biological studies of PET and our data can shed light on the positron penetration in these materials. Our considerations lead to the conclusion that the maximal spatial extent of ^{18}F positrons is ca. 1.7 mm. Nevertheless, in real measurements this value can be lowered to ca. 0.4 mm due to the certain background level.

References

1. Achtziger N, Witthuhn W (1997) Deep levels of chromium in 4H-SiC. Mater Sci Eng B 46:333–335
2. De Cremer K, Cornelis R, Strijckmans K, Dams R, Lameire N, Vanholder R (2002) Behaviour of vanadate and vanadium transferrin complex on different anion-exchange columns. Application of *in vivo* 48V-labelled rat serum. J Chromatogr B Anal Technol Biomed Life Sci 775:143–152
3. Derenzo SE (1979) Precision measurements of annihilation point spread distribution for medically important positron emitters. In: Proc of the 5th Int Conf Positron Annihilation, April 1979, Lake Yamanaka, Japan, pp 819–823
4. Dryzek J (2005) Defect depth scanning over the positron implantation profile in aluminum. Appl Phys A 81:1099–1104
5. Dryzek J, Sieracki J (2007) New formula for description of positron implantation profile in condensed matter. Nucl Instrum Methods Phys Res B 258:493–496
6. Dryzek J, Singleton D (2006) Implantation profile and linear absorption coefficients for positrons injected in solids from radioactive sources 22-Na and 68-Ge/68-Ga. Nucl Instrum Methods Phys Res B 252:197–204
7. Eigler NL, Li AN, Whiting JS *et al*. (eds) (1996) Vascular brachytherapy. Nucletron, Veenendall, The Netherlands
8. GEANT4. http://cern.ch/geant4
9. Hichwa RD, Kadrmas D, Watkins GL *et al*. (1995) Vanadium-48: a renewable source of transmission scanning with PET. Nucl Instrum Methods Phys Res B 99:804–806
10. Levin CS, Hoffman EJ (1999) Calculation of positron range and its effect on the fundamental limit of positron emission tomography system spatial resolution. Phys Med Biol 44:781–799
11. Palmer MR, Zhu XZ, Parker JA (2005) Modeling and simulation of positron range effects for high resolution PET imaging. IEEE Trans on Nuclear Science 52:1391–1395
12. Rorat E, Petelenz B, Marczewska B, Ochab E (2005) Thermoluminescence dosimetry of model line sources containing vanadium-48. Radiat Meas 39:495–501
13. Treurniet JA, Rogers DWO (1999) EGS Windows 4.0 user's manual. NRCC Report PIRS-669. http://www.irs.inms.nrc.ca/inms/EGS_Windows/distribution.html